Title

In vivo comparison of tantalum, tungsten, and bismuth enteric contrast agents to complement intravenous iodine for double-contrast dual-energy CT of the bowel

Journal

Contrast Media & Molecular Imaging, 11(4)

ISSN

1555-4309

Authors

Rathnayake, Samira
Mongan, John
Torres, Andrew S
et al.

Publication Date

2016-07-01

DOI

10.1002/cmmi.1687

Peer reviewed

Published in final edited form as:

Contrast Media Mol Imaging. 2016 July ; 11(4): 254–261. doi:10.1002/cmmi.1687.

In vivo comparison of tantalum, tungsten, and bismuth enteric contrast agents to complement intravenous iodine for double-contrast dual-energy CT of the bowel

Samira Rathnayake, MD[1], **John Mongan, MD, PhD**[1], **Andrew S. Torres, PhD**[2], **Robert Colborn, PhD**[2], **Dong-Wei Gao, MD**[1], **Benjamin M Yeh, MD**[1], and **Yanjun Fu, PhD**[1]

Department of Radiology and Biomedical Imaging, University of California San Francisco (UCSF), 505 Parnassus Avenue, San Francisco, CA 94143-0628

Abstract

To assess the ability of dual-energy CT (DECT) to separate intravenous contrast of bowel wall from intraluminal contrast, we scanned 16 rabbits on a clinical DECT scanner: n=3 using only iodinated intravenous contrast; and n=13 double-contrast enhanced scans using iodinated intravenous contrast and experimental enteric non-iodinated contrast agents in the bowel lumen (5 bismuth-, 4 tungsten-, and 4 tantalum-based). Representative image pairs from conventional CT images and DECT iodine density maps of small bowel (116 pairs from 232 images) were viewed by four abdominal imaging attending radiologists to independently score each comparison pair on a visual analog scale (−100 to +100%) for: 1) preference in small bowel wall visualization; and 2) preference in completeness of intraluminal enteric contrast subtraction. Median small bowel wall visualization was scored 39 and 42 percentage points (95% CI: 30–44% and 36–45%, p<0.001 both) higher at double-contrast DECT than at conventional CT with enteric tungsten and tantalum contrast, respectively. Median small bowel wall visualization at double-contrast DECT was scored 29 and 35 percentage points (95% CI: 20–35% and 33–39%, p<0.001 both) higher with enteric tungsten and tantalum, respectively, than with bismuth contrast. Median completeness of intraluminal enteric contrast subtraction in double-contrast DECT iodine density maps was scored 28 and 29 percentage points (95% CI: 15–31% and 28–33%, p<0.001 both) higher with enteric tungsten and tantalum, respectively, than with bismuth contrast. Results suggest that *in vivo* double-contrast DECT with iodinated intravenous and either tantalum- or tungsten-based enteric contrast provide better visualization of small bowel than conventional CT.

Keywords

Dual-energy CT; CT Enterography; Contrast Agent; Tungsten; Bismuth; Tantalum; Small Bowel

Address for co-correspondence: Benjamin Yeh and Yanjun Fu, Department of Radiology and Biomedical Imaging, University of California San Francisco, Box 0628, M-372, 505 Parnassus Avenue, San Francisco, CA 94143-0628, Tel: 415-353-1821, Fax: 415-476-0616, Ben.Yeh@ucsf.edu and yanjun.fu@gmail.com.

[1]UCSF Department of Radiology and Biomedical Imaging.

[2]General Electric Global Research Center.

For the remaining authors none were declared.

Introduction

Accurate and reliable evaluation of small bowel remains a clinical challenge. Conventional endoscopy does not evaluate the distal small bowel. Capsule endoscopy is relatively time-consuming and may misassign the location of findings (1,2). Fluoroscopic evaluation does not assess bowel wall vascularity.

By contrast, computed tomography (CT) is beneficial in small bowel imaging because it evaluates the entire length of the small bowel and provides multi-planar image display. A major limitation of abdominal CT is that the bowel contrast agents are either “positive” (radiodense) or “neutral” (water attenuation). Positive oral CT contrast material helps differentiate bowel from non-bowel soft tissue and fluid and helps detect bowel leakages or obstructions (3,4). Unfortunately, positive oral contrast material may obscure bowel wall hyper-enhancement as is seen with inflammation, or conversely, lack of bowel wall enhancement, as is seen with ischemia (5). Findings related to bowel wall enhancement are crucial to the evaluation of bowel inflammation, vascular disease, tumors, gastrointestinal bleeding, and ischemia (3,6,7). Neutral enteric contrast is used in conjunction with intravenous contrast for superior visualization of small bowel wall enhancement (CT enterography) because it allows the intravascular iodinated contrast agent signal in the bowel wall to stand out. Unfortunately, neutral enteric contrast is less useful than positive contrast for the detection of intra-abdominal abscesses or bowel leakage because the signal intensity of neutral enteric contrast resembles that of other bodily fluids.

Dual energy CT (DECT) is now increasingly available and allows one to distinguish the signal from different materials if they have distinctly different ratios of X-ray attenuation coefficients at low versus high kVp (peak kilovoltage), even if these materials might have similar attenuation numbers at conventional CT (8,9). Use of a small bowel luminal contrast material that can be digitally separated from conventional intravenous iodinated CT contrast material by DECT could combine the advantages of both positive and neutral oral contrast-enhanced imaging in a single scan, improving the diagnostic evaluation of small bowel.

The ability of DECT to separate selected contrast materials depends on differences in the ratios of X-ray attenuation coefficients at low and high energy between the selected contrast materials. A major limitation of our currently available clinical contrast agents is that they are all based on iodine and barium – these two materials have similar low to high kVp attenuation ratios (hereafter referred to as “attenuation ratios”) and their signals cannot be reliably separated at clinical DECT (8). High-atomic-number elements attenuate X-rays well, and many of these elements have been explored in the past as potential X-ray or CT imaging contrast agents, including bismuth, gold, cesium, tin, tantalum, tungsten and lanthanides (9–19). Representative contrast compounds include: prototypic tantalum oxide colloids described as intravenous X-ray contrast agents in dogs and rabbits in 1972 (11), well-defined tantalum oxide nanoparticles recently used as intravenous contrast agents for CT (10,14), tungsten cluster compounds as intravenous contrast agents for CT (19), bismuth sulfide nanoparticles for blood pool imaging (17), and organic bismuth compound-encapsulated polymeric nanoparticles for both intravascular thrombosis imaging and spectral CT imaging applications (9–19).

For the present study, bismuth, tungsten, and tantalum are chosen for their property of having low to high kVp attenuation ratios substantially different from that of iodine or barium, allowing for possible separation of their signal from iodine and barium at DECT, as well as their potential biocompatibility for use as enteric agents (9,20). Bismuth in particular is currently used in an over-the-counter medication (Pepto-Bismol), and tungsten and tantalum compounds or metals have been used as preclinical oral agents and in implanted medical devices (18,21). Tungsten oxide and especially tantalum oxide are known to be chemically inert at body temperature and pH 2 – 8, which is the expected pH range of human GI tract (4,9).

The comparative abilities of novel bismuth-, tungsten-, and tantalum-based enteric contrast agents to be digitally separated from an intravascular iodinated contrast agent have not been previously described *in vivo.* Our present study investigates whether double-contrast enhanced DECT, with intravenous iodinated contrast and unconventional enteric contrast materials based on bismuth, tungsten, or tantalum can improve bowel wall visualization compared to conventional CT.

Results and Discussion

Example images of double-contrast conventional and DECT are shown in Figures 1–4. Small bowel wall visualization on double-contrast DECT with enteric contrast subtraction was superior to double-contrast conventional CT when enteric tungsten or tantalum was used (median improvement in small bowel wall visualization score of 39 percentage points [95% CI: 30% to 44%,] $p<0.001$, and 42 percentage points [95% CI: 36% to 45%], $p<0.001$, respectively). When enteric bismuth was used with double-contrast DECT, no significant improvement in small bowel wall visualization over double-contrast conventional CT was found (95% CI: −12% to 9%, $p=0.67$) (Figure 5). In our study, the term “conventional CT images” refers to 70 keV virtual monochromatic images reconstructed from the same DECT scan data, which approximate the appearance of a conventional CT scan obtained at 120 kVp. Direct comparisons between individual enteric contrast agents at double-contrast DECT (Figure 6) showed that enteric tungsten and tantalum were superior to enteric bismuth for both small bowel wall visualization (median improvement in visualization score of 29 percentage points [95% CI: 20% to 35%], $p<0.001$ and 35 percentage points [95% CI: 33% to 39%], $p<0.001$, respectively) and enteric contrast subtraction (median improvement in completeness of intraluminal enteric contrast subtraction score of 28 percentage points [95% CI: 15% to 31%], $p<0.001$ and 29 percentage points [95% CI: 28% to 33%], $p<0.001$), respectively). A reader preference was not found in small bowel wall visualization (95% CI: −14% to 8%, $p=0.29$) or completeness of enteric contrast subtraction from small bowel lumen (95% CI: −5% to 0%, $p=0.27$) in the case where double-contrast DECT with enteric tungsten was compared with double-contrast DECT with enteric tantalum (Figure 5). Median small bowel wall visualization was scored 21 percentage points higher (95% CI: 8% to 29%, $p<0.001$) for intravenous contrast-only conventional CT than double-contrast DECT with the use of enteric bismuth contrast material (Figures 4, 5). No significant difference was found in small bowel wall visualization score in the case where intravenous contrast-only conventional CT was compared with double-contrast DECT when enteric tungsten (95% CI: −5% to 1%, $p=0.13$) or enteric tantalum (95% CI: −21% to 6%, $p=0.23$) was used

(Figure 4, 5). Of note, Figures 5 and 6 show a partial visual analog scale (−50% to +50%) since our results fall in this range.

Our *in vivo* animal model study showed that simultaneously administered iodinated intravenous and high-Z (atomic number) enteric contrast agent allows for significantly better visualization of small bowel wall at DECT than at conventional CT. We found that bowel wall visualization was significantly improved (in the case of enteric tantalum or tungsten) on double-contrast DECT iodine density maps compared to double-contrast conventional CT (70 keV images) despite the presence of radiodense oral contrast media, which normally obscures intravascular contrast agent enhancement of the bowel wall at conventional CT (5).

Among these three experimental high-Z enteric agents, we found that a tantalum- or tungsten-based enteric contrast agent provided superior separation from intravenous iodinated agents at double-contrast DECT than did a bismuth-based enteric contrast agent. Iodine density maps obtained from DECT scans with tantalum or tungsten enteric agents showed significantly better small bowel wall visualization and better quality of subtraction of enteric contrast than when a bismuth-based enteric agent was used.

These differences in visualization and enteric contrast subtraction at DECT may be explained by the differences between the low to high kVp attenuation ratios of each enteric/intravenous contrast agent pair used for our study. Iodine, bismuth, tantalum, and tungsten are known to have 80:140 kVp CT number attenuation ratios of approximately 1.7, 1.3, 1.0, and 1.0, respectively (4,9,20,22). Of note, the attenuation ratios of materials depend on the specific X-ray spectra of scanners including use of beam filters. It is known that noise for DECT material separation is inversely proportional to the difference of low to high kVp attenuation ratios between the two materials being separated (23). Since the low to high kVp CT number attenuation ratio of bismuth (1.3) is closer to that of iodine (1.7) than are those of tantalum (1.0) or tungsten (1.0), separation of bismuth from iodine can be expected to be relatively noisier than separation of tantalum from iodine, or tungsten from iodine. Our in vivo results build on those of recently published in vitro studies on DECT imaging of non-iodinated agents (20,24).

A major limitation of conventional CT enterography is that the bowel lumen must be either neutral (no bright oral contrast given) or bright (positive iodine or barium contrast given). Absence of bright oral contrast allows evaluation of abnormalities in intravenous enhancement of the bowel wall, but results in decreased sensitivity for abscess or other extralumenal fluid because such fluid collections may resemble neutral signal bowel lumen. Conversely, presence of bright oral contrast adversely interferes with evaluation of bowel wall enhancement, but allows superior identification of abscess or other extralumenal fluid collections, which contain unenhanced (neutral signal) fluid.

Our results suggest that appropriately selected contrast agent combinations for DECT could simultaneously provide the diagnostic benefits of a positive enteric contrast scan to mark the bowel lumen and, at the same time, also allow evaluation of bowel wall enhancement on iodine density maps that remove the positive lumenal signal. Powerful imaging by double-contrast DECT could thus be particularly valuable for inflammatory conditions of the bowel,

where identification of extralumenal collections (best seen when the bowel lumen is bright) and evaluation of hyper- or hypoenhancement of the bowel wall (best seen when the bowel lumen is dark) are both of concern.

Our study has several limitations. First, 70 keV virtual monochromatic images were used to represent conventional CT images in lieu of traditional single-energy scans at 120 kVp. While this is an approximation, it allows images to be produced that are identical except for the technique (DECT density map versus “conventional” virtual monochromatic), which eliminates variables of positioning and contrast phase timing that would otherwise complicate the comparison. Second, the radiologists were presented with fixed images rather than full CT image series on a PACS system. Although this represents a deviation from clinical practice, this also served to limit spurious variability by ensuring that each radiologist was evaluating the wall of the same portion of bowel. Had our study been focused on the diagnosis of small bowel pathology, evaluation of a full CT image series on a PACS system may have been more fitting.

An additional limitation is that, while our experiment shows that normal bowel wall is clearly visualized with double-contrast DECT iodine density map images, we have not yet determined how robust this technique would be in the evaluation of bowel pathology. Qu *et al.* have studied a small bowel phantom containing simulated polyps with varying degrees of enhancement and a bismuth-based enteric contrast agent in bowel lumen. This study showed a higher rate of polyp detection with DECT than with routine CT technique (4). Further studies continuing our initial *in vivo* evaluation of double-contrast DECT will be needed to assess the value of this technique for the evaluation of bowel disease with experimental DECT contrast agents in animal models, and are also essential to stimulate the development of clinically-feasible enteric contrast material for DECT.

Development and regulatory approval of double-contrast DECT will require further development and testing of a safe enteric contrast agent with favorable X-ray attenuation characteristics. Currently, none of the contrast materials approved by the United States Food and Drug Administration has a low to high kVp attenuation ratio that is suitable for material separation from iodinated agents at double-contrast enhanced DECT. Our work provides proof of concept that double-contrast DECT with novel enteric contrast agents can potentially add value to bowel imaging. Tungsten and tantalum metals are known to be relatively inert; and further bismuth salts, tungsten oxide clusters, and particularly tantalum oxides have been used in the past as experimental radiographic contrast agents in gastrointestinal examinations and are considered to be among suitable candidates for development (10,12,13,25,26).

Conclusions

In summary, we found that iodine density maps from *in vivo* double-contrast DECT scans allowed for better small bowel wall visualization than did conventional CT when tantalum- or tungsten-based enteric contrast agents were used. Further, the completeness of enteric contrast subtraction from the small bowel lumen and small bowel wall visualization on DECT iodine density maps were better when images were obtained with a tantalum- or

tungsten-based enteric contrast agent than with a bismuth-based enteric agent. Our results will help inform the selection and further development of novel non-iodinated, non-barium contrast materials for clinical application to achieve the full potential of dual energy CT, and could dramatically improve the diagnostic yield of CT over what we are currently able to obtain with merely iodine and barium contrast agents.

Experimental

Animal subjects

Approval from the Institutional Animal Care and Use Committee was obtained, and NIH guidelines for care and use of laboratory animals were observed. Thirteen female New Zealand White rabbits (Western Oregon Rabbit, Co, Philomath, OR) weighing between 3.7 and 4.3 kg were used.

Anesthesia

For CT scans, anesthesia of each animal was separately induced with 35 mg/kg Ketamine (Ketaset, Fort Dodge Animal Health, Fort Dodge, IA) and 3 mg/kg Xylazine (Spectrum, New Brunswick, NJ) by intramuscular injection and maintained under general anesthesia with 2–4% inhaled isoflurane (Summit Anesthesia Equipment, Foster City, CA).

Contrast agents

Iohexol (Omnipaque™, 350 mgI/ml, GE Healthcare Inc, Princeton, NJ) was used as the intravenous contrast agent. All enteric contrast materials were chosen to produce about 400 HU at 120 kVp tube potential. A bismuth-containing suspension (Pepto Bismol®, Procter & Gamble, Cincinnati, Ohio) containing 17.5 mg bismuth subsalicylate per mL (thus 10.1 mg bismuth per mL) was used as enteric contrast without further modification. Tungsten oxide (WO_3) nanoparticles (Nanostructured and Amorphous Materials, Houston, Texas) were suspended in a sterile 3 w/v % D-sorbitol solution just before oral administration as an experimental enteric contrast agent, in a concentration of 16 mg tungsten per ml. Tantalum oxide (Ta_2O_5) nanoparticles (GE Global Research Center, Niskayuna, New York) or tantalum oxide powder (Sigma-Aldrich, St. Louis, Missouri) which was similar to these nanoparticles in X-ray attenuation profile were dispersed in a sterile 3 w/v % D-sorbitol solution just before oral administration as an experimental enteric contrast agent, in the concentration of 16 mg tantalum per mL. These specific concentrations for bismuth, tungsten, and tantalum agents are chosen purposefully to match with one another on the CT attenuation number for fair imaging comparison.

It is well documented that CT number of a given contrast agent (calibrated with water as 0 HU) is linearly directly proportional to its concentration in the common contrast concentration range of clinical scenarios(27,28). Thus the low-to-high kVp attenuation ratio should be independent of contrast agent concentration for any given agent because the concentration factor is certainly cancelled in the calculation of this attenuation ratio. Similarly, the difference of attenuation ratios of two contrast agents is also independent of their concentrations.

Intravenous-contrast-only dual energy CT scans

Three of the rabbits were initially scanned with intravenous iohexol contrast only, without receiving any enteric contrast agent. Iohexol 700mg I/kg (Omnipaque 350™, GE Healthcare Inc, Princeton, NJ; dose 2 mL/kg body weight) was delivered as a bolus via an intravenous catheter placed in an auricular vein 15 seconds prior to CT imaging. The scans were obtained with a rapid kVp switching dual energy CT scanner Discovery CT750 HD (GE Healthcare, Milwaukee, Wisconsin) in dual-energy (GSI) mode protocol GSI-11 (medium filter, 0.8-second rotation time, 40-mm collimation) and 0.625 mm slice thickness for each of the three rabbits. Axial and coronal 70 keV virtual monochromatic images, which simulate 120 kVp conventional CT images, were reconstructed at the console. These three rabbits were then recovered and given at least two days for intravenous contrast to clear before additional imaging.

Double-contrast dual energy CT scans

For each rabbit, oral contrast was administered by gastric gavage using a 12 Fr pediatric orogastric tube. Five of the rabbits each received 180 mL of bismuth subsalicylate suspension (Pepto-Bismol, Procter & Gamble, Cincinnati, Ohio). Four rabbits each received 180 mL of tungsten oxide nanoparticle suspension (16 mg tungsten/mL) in 3% sorbitol solution and four rabbits received 180 mL of tantalum oxide powders (or equivalent density nanoparticles as reported by Torres et al in 2012 (18); 16 mg Ta/mL) in 3% sorbitol. The orogastric tube was removed after enteric contrast administration.

Twenty minutes after enteric contrast administration, rabbits were anesthetized. Then intravenous Iohexol 700 mg I/kg was given as a bolus via an auricular vein catheter 15 seconds prior to CT imaging with a Discovery CT750 HD scanner (GE Healthcare, Milwaukee, Wisconsin) in dual-energy (GSI) mode. The scans were obtained with protocol GSI-11 (medium filter, 0.8-second rotation time, 40-mm collimation) and 0.625 mm slice thickness for each of the 13 rabbits. Axial and coronal 70 keV virtual monochromatic images, which simulate 120 kVp conventional CT images, as well as iodine material density map reconstructions were generated (29). Of note, our version of this software is limited to basis materials that do not have a k-edge between 40 and 140 keV (Saad Sirohey, PhD [GE Healthcare], written communication, June 2012). Therefore, for iodine/bismuth material decomposition, we used empirically determined X-ray attenuation coefficients in the GSI viewer software to simulate a material with the same low to high kVp attenuation ratio as bismuth but without a k-edge. For rabbits that received enteric tungsten (or enteric tantalum) and intravenous iodine, the iodine/water material decomposition basis was used to generate iodine material density maps since the attenuation ratios of tungsten and tantalum are very similar to that of water. Of note, for the iodine/bismuth material decomposition, air appears very bright (Figure 1-B and Figure 4-B) due to the limitations of currently available software conducting material decomposition with a basis set of only two materials, in the particular cases that the attenuation ratio of a base material (like Bismuth here) is considerably greater than 1.0. Two material decomposition attempts to dichotomize the CT “signal” from each voxel as being composed of only the two materials in the equation. When both materials have low to high kVp attenuation ratios significantly higher than 1.0, then the only way in which a material like air (defined as having an attenuation ratio of 1.0) can be represented

and mathematically solved by the assignment of a hypothetically large magnitude positive concentration of one material offset by a large magnitude “negative calculated concentration” of the other material. In the case of iodine density maps for bismuth/iodine decomposition, the algorithm results in false high iodine values for air on the iodine density maps. This artifact may be eliminated with a multi-material decomposition algorithm instead of a two-material decomposition algorithm in this particular case, but has not been implemented in available software. The artifact is not observed in decompositions involving tungsten or tantalum because both of these elements have attenuation ratios very close to 1.0 which is for water.

Image evaluation

From the 70 keV virtual monochromatic (“conventional CT”) images and the iodine density map images (“DECT”) generated in the 13 double-contrast DECT scans, and from the conventional CT images of 3 intravenous-contrast-only scans, representative small bowel wall and small bowel lumen images were chosen to generate pairs of images for the following comparisons: double-contrast conventional CT versus DECT iodine density maps for each enteric contrast agent tested, conventional CT with intravenous contrast alone versus DECT iodine density maps for each enteric contrast agent tested, and small bowel wall visualization/completeness of subtraction of small bowel lumen between DECT iodine density maps when one enteric contrast agent was present versus when another enteric contrast agent was present (Table 1). Images were selected by radiologists who performed the rabbit-imaging portion of the study such that the small bowel wall visualization and completeness of small bowel lumen subtraction were representative of the image set. Each respective image series was optimally windowed and leveled to highlight the small bowel, and the chosen window/level was the same across each image category. Within each image category, generated images were randomly chosen and paired with a comparison image on a slide. The randomization was constrained such that any two scans were only compared once. The placement of the image on the left and right side of each slide was randomized for each pair, and the order of slides in the final presentation was additionally randomized with a randomized sequence generator. 116 comparison pairs of small bowel images were generated in total.

Image pairs were presented to 4 sub-specialty trained abdominal imaging attending radiologists (11, 7, 5, and 4 years of experience) who were otherwise not involved with the animal scans. Each radiologist independently assessed all 116 slides (comparison pairs) and marked their evaluation scores based on a visual analog scale. The leftmost point on the preference scale (−100%) was defined to the radiologists as absolute preference of the left-sided image; the rightmost point (+100%) was defined as absolute preference of the right-sided image; the central point (0%) was defined as equal preference of both images of the comparison pair. Radiologists were instructed to score the relative preference for small bowel wall visualization and relative completeness of intraluminal enteric contrast subtraction for each comparison pair presented.

Analysis

Data from the response sheets were tabulated and analyzed with a Shapiro-Wilk test for normality of distribution (p values ranged from 0.29–0.72, and none were significant), followed by a Wilcoxon Signed Rank test for comparisons of ordinal measures using a statistical software package (R, version 2.14; R Development Core Team, Vienna, Austria). Accordingly, results for each comparison are provided in terms of median improvement in visualization of small bowel wall score and median improvement in subtraction of contrast from bowel lumen score with appropriate confidence intervals. Fleiss Kappa statistics was calculated for each comparison (Table 1). Values were noted to range from the low negative to low positive range (−0.11 to 0.09), indicating that there was poor agreement between each of the four radiologist readers who scored images in the study, and reflecting that there was substantial inter-observer variation in ratings on the visual analogue scale. Data on image preference for small bowel wall visualization and for completeness of small bowel lumen subtraction were analyzed with results for all readers pooled. Because readers were looking at specific designated image features rather than reading complete studies, it was not necessary to correct for within-animal correlation. A p value of 0.05 was used as the threshold for statistical significance.

Acknowledgments

Sources of Funding: SR is a Howard Hughes Medical Institute Medical Research Fellow. JM is supported by NIBIB T32 Training Grant 1 T32 EB001631. YF and BMY are supported by NIH grants R21EB013816, 1R01EB015476, and R01CA122257. BMY has ongoing grants from GE Healthcare. AST and RC are supported by NIH grant R01EB015476.

This work was funded in part by the National Institutes of Health (grant nos. R21EB013816, R01EB015476 and R01CA122257) and the National Institute of Biomedical Imaging and Bioengineering (grant no. T32 EB001631). We also thank Amy Chiyuan Zhang for assistance with the statistical analysis.

References

1. Lewis BS, Swain P. Capsule endoscopy in the evaluation of patients with suspected small intestinal bleeding: Results of a pilot study. Gastrointestinal endoscopy. 2002; 56(3):349–353. [PubMed: 12196771]
2. Voderholzer WA, Beinhoelzl J, Rogalla P, Murrer S, Schachschal G, Lochs H, Ortner MA. Small bowel involvement in Crohn’s disease: a prospective comparison of wireless capsule endoscopy and computed tomography enteroclysis. Gut. 2005; 54(3):369–373. [PubMed: 15710985]
3. Paulsen SR, Huprich JE, Fletcher JG, Booya F, Young BM, Fidler JL, Johnson CD, Barlow JM, Earnest F. CT enterography as a diagnostic tool in evaluating small bowel disorders: review of clinical experience with over 700 cases. Radiographics : a review publication of the Radiological Society of North America, Inc. 2006; 26:641–657. discussion 657–662.
4. Qu M, Ehman E, Fletcher JG, Huprich JE, Hara AK, Silva AC, Farrugia G, Limburg P, McCollough CH. Toward biphasic computed tomography (CT) enteric contrast: material classification of luminal bismuth and mural iodine in a small-bowel phantom using dual-energy CT. Journal of computer assisted tomography. 2012; 36:554–559. [PubMed: 22992606]
5. Jancelewicz T, Vu LT, Shawo AE, Yeh B, Gasper WJ, Harris HW. Predicting strangulated small bowel obstruction: an old problem revisited. Journal of gastrointestinal surgery : official journal of the Society for Surgery of the Alimentary Tract. 2009; 13(1):93–99. [PubMed: 18685902]
6. Fishman EK, Wolf EJ, Jones B, Bayless TM, Siegelman SS. CT evaluation of Crohn’s disease: effect on patient management. AJR American journal of roentgenology. 1987; 148(3):537–540. [PubMed: 3492882]

7. Raptopoulos V, Schwartz RK, McNicholas MM, Movson J, Pearlman J, Joffe N. Multiplanar helical CT enterography in patients with Crohn's disease. AJR American journal of roentgenology. 1997; 169(6):1545–1550. [PubMed: 9393162]
8. Anderson NG, Butler AP, Scott NJ, Cook NJ, Butzer JS, Schleich N, Firsching M, Grasset R, de Ruiter N, Campbell M, Butler PH. Spectroscopic (multi-energy) CT distinguishes iodine and barium contrast material in MICE. European radiology. 2010; 20(9):2126–2134. [PubMed: 20309554]
9. Mongan J, Rathnayake S, Fu Y, Wang R, Jones EF, Gao DW, Yeh BM. In Vivo Differentiation of Complementary Contrast Media at Dual-Energy CT. Radiology. 2012; 265(1):267–272. [PubMed: 22778447]
10. Bonitatibus PJ Jr, Torres AS, Goddard GD, FitzGerald PF, Kulkarni AM. Synthesis, characterization, and computed tomography imaging of a tantalum oxide nanoparticle imaging agent. Chem Commun (Camb). 2010; 46(47):8956–8958. [PubMed: 20976321]
11. Gianturco C, Ruskin B, Steggerda FR, Takeuchi T. A feasibility study of splenohepatography with tantalum metal and tantalum pentoxide. Radiology. 1972; 102(1):195–196. [PubMed: 5061767]
12. Goldberg HI, Dodds WJ, Jenis EH. Experimental esophagitis: roentgenographic findings after insufflation of tantalum powder. The American journal of roentgenology, radium therapy, and nuclear medicine. 1970; 110(2):288–294.
13. Margulis AR, Stoughton JA, Stein LA. Non-contractile movement of tantalum powder in the canine rectum. The American journal of roentgenology, radium therapy, and nuclear medicine. 1975; 125(1):244–250.
14. Oh MH, Lee N, Kim H, Park SP, Piao Y, Lee J, Jun SW, Moon WK, Choi SH, Hyeon T. Large-scale synthesis of bioinert tantalum oxide nanoparticles for X-ray computed tomography imaging and bimodal image-guided sentinel lymph node mapping. Journal of the American Chemical Society. 2011; 133(14):5508–5515. [PubMed: 21428437]
15. Pan D, Roessl E, Schlomka JP, Caruthers SD, Senpan A, Scott MJ, Allen JS, Zhang H, Hu G, Gaffney PJ, Choi ET, Rasche V, Wickline SA, Proksa R, Lanza GM. Computed tomography in color: NanoK-enhanced spectral CT molecular imaging. Angewandte Chemie. 2010; 49(50):9635–9639. [PubMed: 21077082]
16. Pan D, Williams TA, Senpan A, Allen JS, Scott MJ, Gaffney PJ, Wickline SA, Lanza GM. Detecting vascular biosignatures with a colloidal, radio-opaque polymeric nanoparticle. Journal of the American Chemical Society. 2009; 131(42):15522–15527. [PubMed: 19795893]
17. Rabin O, Manuel Perez J, Grimm J, Wojtkiewicz G, Weissleder R. An X-ray computed tomography imaging agent based on long-circulating bismuth sulphide nanoparticles. Nature materials. 2006; 5(2):118–122. [PubMed: 16444262]
18. Torres AS, Bonitatibus PJ Jr, Colborn RE, Goddard GD, Fitzgerald PF, Lee BD, Marino ME. Biological performance of a size-fractionated core-shell tantalum oxide nanoparticle x-ray contrast agent. Investigative radiology. 2012; 47(10):578–587. [PubMed: 22836312]
19. Yu SB, Droege M, Downey S, Segal B, Newcomb W, Sanderson T, Crofts S, Suravajjala S, Bacon E, Earley W, Delecki D, Watson AD. Dimeric W3SO3 cluster complexes: synthesis, characterization, and potential applications as X-ray contrast agents. Inorganic chemistry. 2001; 40(7):1576–1581. [PubMed: 11261967]
20. Falt T, Soderberg M, Wasselius J, Leander P. Material Decomposition in Dual-Energy Computed Tomography Separates High-Z Elements From Iodine, Identifying Potential Contrast Media Tailored for Dual Contrast Medium Examinations. Journal of computer assisted tomography. 2015; 39(6):975–980. [PubMed: 26295191]
21. Bonitatibus PJ Jr, Torres AS, Kandapallil B, Lee BD, Goddard GD, Colborn RE, Marino ME. Preclinical assessment of a zwitterionic tantalum oxide nanoparticle X-ray contrast agent. ACS nano. 2012; 6(8):6650–6658. [PubMed: 22768795]
22. Mongan J, Rathnayake S, Fu Y, Gao DW, Yeh BM. Extravasated contrast material in penetrating abdominopelvic trauma: dual-contrast dual-energy CT for improved diagnosis--preliminary results in an animal model. Radiology. 2013; 268(3):738–742. [PubMed: 23687174]

23. Primak, aN; Ramirez Giraldo, JC.; Liu, X.; Yu, L.; McCollough, CH. Improved dual-energy material discrimination for dual-source CT by means of additional spectral filtration. Medical physics. 2009; 36:1359–1369. [PubMed: 19472643]

24. Gabbai M, Leichter I, Mahgerefteh S, Sosna J. Spectral material characterization with dual-energy CT: comparison of commercial and investigative technologies in phantoms. Acta radiologica. 2015; 56(8):960–969. [PubMed: 25182803]

25. Koutsospyros, a; Braida, W.; Christodoulatos, C.; Dermatas, D.; Strigul, N. A review of tungsten: from environmental obscurity to scrutiny. Journal of hazardous materials. 2006; 136:1–19. [PubMed: 16343746]

26. Patton DD. Insight on the radiologic centennial: a historical perspective. Part 4. Of gastrointestinal radiology, bread and butter; or, the flowering of barium sulfate. Investigative radiology. 1994; 29(4):472–479. [PubMed: 8034456]

27. Mullan BF, Madsen MT, Messerle L, Kolesnichenko V, Kruger J. X-ray attenuation coefficients of high-atomic-number, hexanuclear transition metal cluster compounds: a new paradigm for radiographic contrast agents. Academic radiology. 2000; 7(4):254–259. [PubMed: 10766098]

28. Yu SB, Watson AD. Metal-Based X-ray Contrast Media. Chemical reviews. 1999; 99(9):2353–2378. [PubMed: 11749484]

29. Kessler, JRJ.; Ellestad, M.; Pawha, P.; Doshi, A.; Stein, EG.; Tanenbaum, LN. Dual Energy Spectral CT (DESCT) Allows Selection of the Optimal Monochromatic Energy for Imaging the Instrumented Spine and Improves Diagnostic Quality over Traditional Imaging. RSNA Annual Meeting; Chicago, IL. 2010;

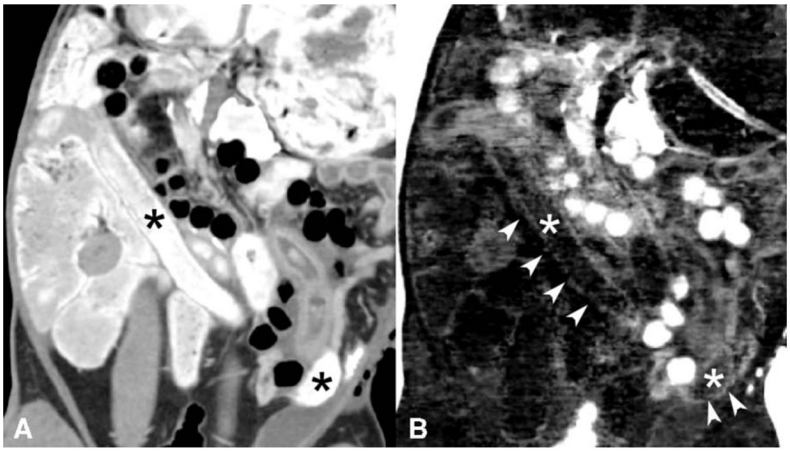

Figure 1.

Simultaneous enteric bismuth (Bi) contrast and intravenous iodine contrast in a rabbit model. Conventional CT image (A) shows bright enteric bismuth contrast in the bowel lumen (*) that limits visualization of the curvilinear bowel wall enhanced by intravenous iodine. The DECT iodine density map (B) shows partial subtraction of bismuth enteric contrast (*), but the curvilinear bowel wall enhancement from iodine (arrowheads) is not well seen. The DECT iodine map image was not significantly preferred over the co-registered conventional CT image in regards to small bowel wall visualization. Note also that air appears bright on the iodine/bismuth material decomposition (B) due to a current software-associated air artifact, further detailed in the methods section.

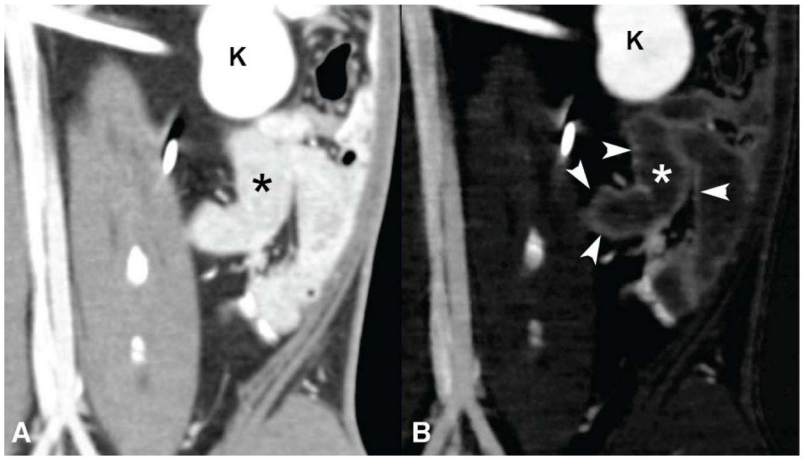

Figure 2.

Simultaneous enteric tungsten (W) contrast and intravenous iodine contrast in a rabbit model. Conventional CT image (A) shows bright enteric tungsten contrast in the bowel lumen (*) that limits visualization of the curvilinear bowel wall enhanced by intravenous iodine. The iodine density image map (B) from DECT shows improved small bowel wall (arrowheads) visualization compared to the co-registered image from the simulated conventional CT (A). * = bowel lumen, which is bright in the simulated conventional CT image due to tungsten contrast, but is dark in the iodine density image where the tungsten contrast is subtracted. K=kidney.

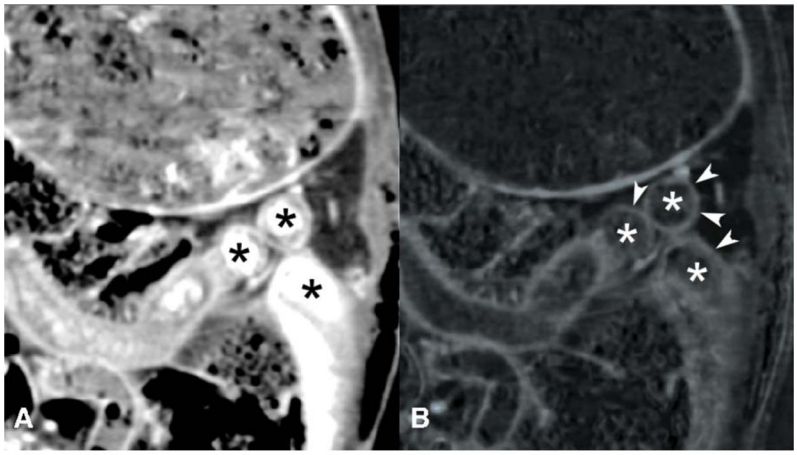

Figure 3.

Simultaneous enteric tantalum (Ta) contrast and intravenous iodine contrast in a rabbit model. Conventional CT image (A) shows bright enteric tantalum contrast in the bowel lumen (*) that limits visualization of the curvilinear bowel wall enhanced by intravenous iodine. The iodine density image map (B) from DECT shows improved small bowel wall (arrowheads) visualization compared to the co-registered image from the conventional CT (A). * = bowel lumen, which is bright in the conventional CT image due to tantalum contrast, but is dark in the iodine density image where the tantalum contrast is subtracted.

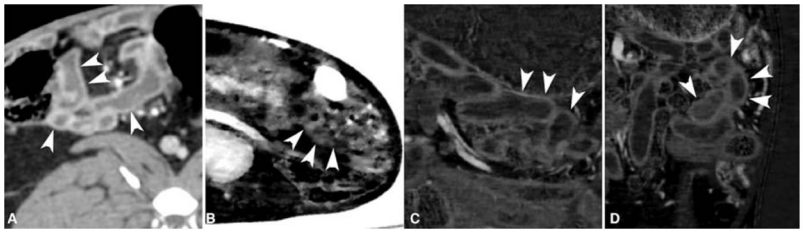

Figure 4.

Representative iodine density map images of small bowel in rabbits enhanced with double-contrast (enteric bismuth or tungsten or tantalum contrast, and intravenous iodine contrast). Small bowel wall (arrowheads) visualization score was significantly better in an intravenous contrast-only conventional CT image (A) than in an iodine density map from enteric bismuth-enhanced double-contrast DECT (B) where the curvilinear bowel wall was indistinct and bowel lumen contrast poorly subtracted. Note that air appears bright on the iodine/bismuth material decomposition (B) due to a software-associated artifact, further detailed in the methods section. Images (C) and (D) are iodine density maps of double-contrast DECT where enteric tungsten and tantalum contrast were used respectively. These latter images show near complete subtraction of the intraluminal tungsten and tantalum contrast, respectively, and vividly show the curvilinear bowel wall enhancement by the intravenous iodinated contrast material. The small bowel wall visualization for the iodine density map of tungsten and tantalum enteric contrast enhanced DECT was comparable with but not significantly preferred over that of intravenous-contrast-only conventional CT (A).

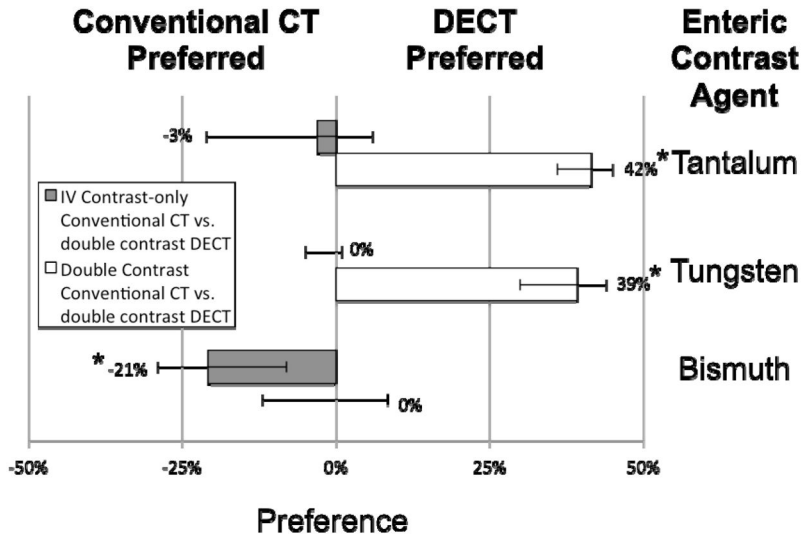

Figure 5.

Pairwise comparison of small bowel wall visualization at conventional CT versus iodine density maps from double-contrast enhanced DECT with enteric bismuth (or tungsten or tantalum) contrast and intravenous iodine contrast in rabbits. Scored median improvement in small bowel wall visualization is shown by bar graph for comparing intravenous-contrast enhanced conventional CT (to the left of the bold line) versus DECT iodine maps (to the right of the bold line) in the case of tantalum, tungsten, and bismuth contrast respectively. Whiskers denote the 95% confidence interval. * = $p < 0.001$

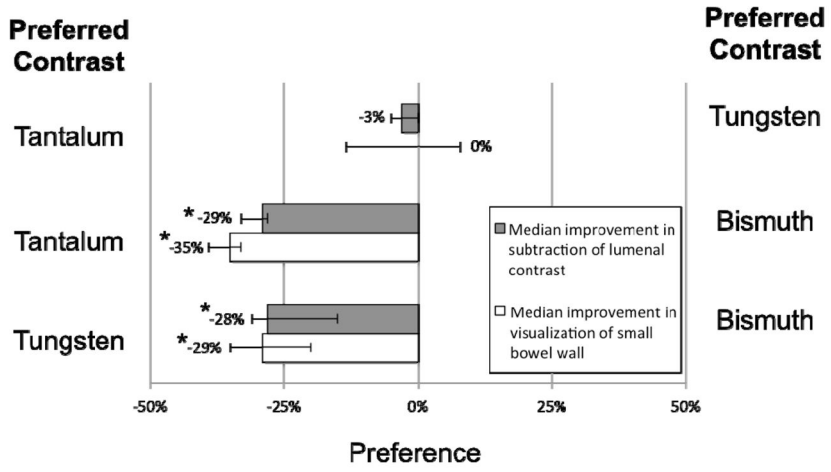

Figure 6.

Pairwise comparison of DECT iodine density maps using three different experimental enteric contrast agents for small bowel evaluation in rabbits. Scored median improvement in small bowel wall visualization and scored median improvement in completeness of intraluminal contrast subtraction are shown for tantalum versus tungsten (top pair), tantalum versus bismuth (middle pair), and tungsten versus bismuth (bottom pair). Whiskers denote the 95% confidence interval. * = $p < 0.001$

Table 1

Rabbit Small Bowel Image Comparison with Different Scan Methods and Contrast Combinations. “Conventional CT” images stand for 70 keV virtual monochromatic images here, which simulate 120 kVp conventional CT. “Conventional CT Pre-oral Contrast” images are 70 keV virtual monochromatic images, which simulate 120 kVp conventional CT, acquired from rabbits that only received intravenous contrast. “I(Bi)” = DECT iodine density map generated with an iodine/bismuth material decomposition basis from rabbits that received enteric bismuth and intravenous iodine. “I(W)” = DECT iodine density map generated with an iodine/water material decomposition basis from rabbits that received enteric tungsten and intravenous iodine. “I(Ta)” = DECT iodine density map generated with an iodine/water material decomposition basis from rabbits that received enteric tantalum and intravenous iodine. Fleiss kappa statistics for strength of inter-observer agreement are shown for each comparison.

Comparison	Image Pairs	Anatomy evaluated	Fleiss Kappa
Conventional CT vs. I(Bi)	9	Small bowel wall visualization	0.058
Conventional CT vs. I(W)	8		−0.049
Conventional CT vs. I(Ta)	9		−0.094
Conventional CT Pre-oral Contrast vs. I(Bi)	10		−0.020
Conventional CT Pre-oral Contrast vs. I(W)	10		−0.042
Conventional CT Pre-oral Contrast vs. I(Ta)	10		−0.066
I(Bi) vs. I(W)	10		−0.011
I(Bi) vs. I(Ta)	10		−0.029
I(W) vs. I(Ta)	10		−0.031
I(Bi) vs. I(W)	10	Completeness of enteric contrast subtraction from the small bowel lumen	−0.110
I(Bi) vs. I(Ta)	10		−0.043
I(W) vs. I(Ta)	10		−0.019

*I(X) = DECT “Iodine-only” density map where X is the enteric contrast agent, either Bi, W, or Ta. Bi = bismuth subsalicylate, W = tungsten oxide, Ta = tantalum oxide